

Synthesis, characterization and catalytic activity of mesoporous trivalent iron substituted aluminophosphates

Ch. Subrahmanyam, B. Viswanathan*, T.K. Varadarajan

Department of Chemistry, Indian Institute of Technology Madras, Chennai 600036, India

Received 27 February 2003; received in revised form 1 March 2004; accepted 5 March 2004

Available online 25 September 2004

Abstract

Trivalent iron incorporated mesoporous aluminophosphate was synthesized under hydrothermal conditions. The synthesized mesoporous Fe-AIPO was characterized by using various physico-chemical techniques, which confirm the formation of mesophase as well as the presence of trivalent iron in the framework. Catalytic activity of mesoporous Fe-AIPO was tested for the oxidation of cyclohexane.

© 2004 Elsevier B.V. All rights reserved.

Keywords: Mesoporous solids; Aluminophosphates; MCM; Cyclohexane; Aerial oxidation

1. Introduction

Saturated hydrocarbons are among the most abundant of all naturally occurring organic molecules and they are the most difficult to oxyfunctionalize at lower temperatures in a controlled manner. With the discovery of microporous aluminophosphates, various transition metal ions have been incorporated into their frameworks and the resulting molecular sieves have been employed as catalysts for selective oxyfunctionalization of alicyclic hydrocarbons [1,2]. Recently, microporous aluminophosphates containing Fe^{3+} , Mn^{2+} and Co^{2+} in the framework have been used for oxidation of cyclohexane [3]. Though, these molecular sieves (zeotypes) have been shown as potential systems for the production of fine chemicals, pore size constraints limit the applications of these materials. With the discovery of M41S by Mobil researchers, it has been made possible to overcome this problem [4]. A few attempts have also been made to synthesize mesoporous aluminophosphates containing transition metal ions [5–11]. In the present study, synthesis and characterization of iron incorporated mesoporous aluminophosphate (Fe-AIPO) are reported. Results on the catalytic activity of Fe-AIPO for the

aerial oxidation of cyclohexane are also discussed. For comparison, the same reaction has been studied over mesoporous Fe-MCM-48.

2. Experimental

2.1. Synthesis of mesoporous Fe-AIPO

Mesoporous iron incorporated aluminophosphates (Fe-AIPO) were synthesized by using cetyl trimethyl ammonium bromide (CTAB) (CDH, AR) as the structure-directing agent. Aluminium hydroxide (SRL, AR) and 85% phosphoric acid were employed as the aluminium and phosphorous sources, respectively. Ferric nitrate nonahydrate was used as iron source. In a systematic procedure, to an aqueous solution of phosphoric acid, aluminium hydroxide was added under vigorous stirring. To this mixture, aqueous solution of ferric nitrate (CDH, AR) was added and stirring was continued further in order to attain homogeneous mixture. To this mixture, surfactant CTAB solution was added and stirred for half an hour. At this stage, tetramethylammonium hydroxide (TMAOH) (25% in water, SRL) was added dropwise to maintain the pH around 9.5. The homogeneous gel thus obtained was found to have the following composition: 0.95

* Corresponding author. Tel.: +91 44 257 8250; fax: +91 44 235 0509.
E-mail address: bviswanathan@hotmail.com (B. Viswanathan).

$\text{Al}_2\text{O}_3:0.05 \text{Fe}_2\text{O}_3:1.00 \text{P}_2\text{O}_5:0.50 \text{CTAB}:300 \text{H}_2\text{O}$. The homogeneous gel was stirred at room temperature for 24 h and autoclaved at 428 K for 24 h. The product was separated, washed with water and oven dried. Calcination was performed in air at 773 K to remove the organic surfactant. Mesoporous Fe-MCM-48 was synthesized according to the procedure reported in one of our earlier communications [10].

2.2. Characterization and catalytic activity of Fe-AlPO

Low-angle X-ray diffraction is the first and foremost technique to confirm the formation of mesophase. The low-angle X-ray diffraction pattern of the sample was recorded on Siemens D 500 ($\theta/2\theta$) using monochromatised Cu $K\alpha$ radiation ($\lambda = 1.5406 \text{ \AA}$) with a scan speed of $1^\circ/\text{min}$ over the range $2 < 2\theta < 10^\circ$. In order to observe the nature of the surfactant and its removal, thermal analysis was used. Thermal analyses of the samples were made with thermal analyzer (Perkin Elmer model TGA 7) at a heating rate of 20 K/min. N_2 adsorption–desorption measurements at 77 K were made using CE instruments, Sorptomatic 1990. UV–vis spectra were recorded in nujol mode on Cary 5E UV-VIS-NIR spectrophotometer. ESR spectra were recorded with Varian E-112 spectrometer at room temperature and also at 77 K. Oxidation of cyclohexane was performed in a high-pressure stainless steel reactor lined with Teflon and dry air was used as oxidant. A pressure of 20 or 30 bar of air was used and the temperature was maintained at 403 K. The duration of the reaction was 24 h. Product identification was carried out with authentic samples and qualitative analysis was done using Nucon-4765 gas chromatograph with SE-30 column. The same reaction was tested over Fe containing silicate analogue Fe-MCM-48. In order to ensure the possible mechanism, the reaction was carried out in presence of small quantity of radical initiator tetrabutyl hydrogen peroxide (TBHP) and radical inhibitor hydroquinone (HQ) and the reaction was continued further.

3. Results and discussion

3.1. XRD

Low-angle XRD patterns confirm the formation of the mesophase of the materials synthesized. Figs. 1 and 2 represent the XRD pattern of the as-synthesised and calcined Fe-AlPO materials, respectively. As-synthesised mesoporous Fe-AlPO shows a maximum intense peak with d -spacing value 35.8 \AA , which corresponds to the 1 0 0 reflection. Upon calcination in air, a decrease in the d_{100} spacing from 35.8 to 34.74 \AA was observed. This decrease is due to the contraction of the unit cell during the calcination. However, the peak intensity remains the same confirming that even after calcination, the materials retained their XRD pattern. These patterns can be indexed to uni-dimensional hexagonal lattice characteristic of MCM-41 type structure. In addition to the

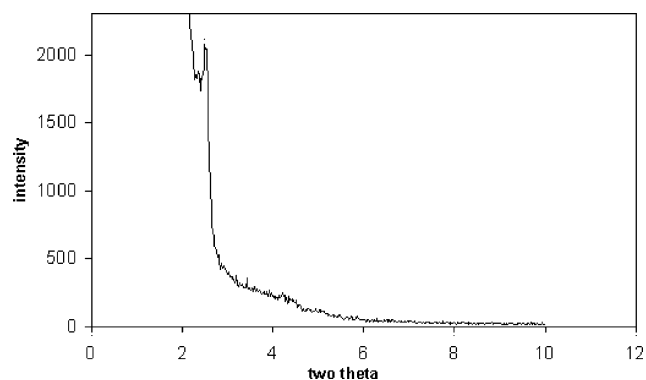


Fig. 1. XRD pattern of mesoporous Fe-AlPO as-synthesized.

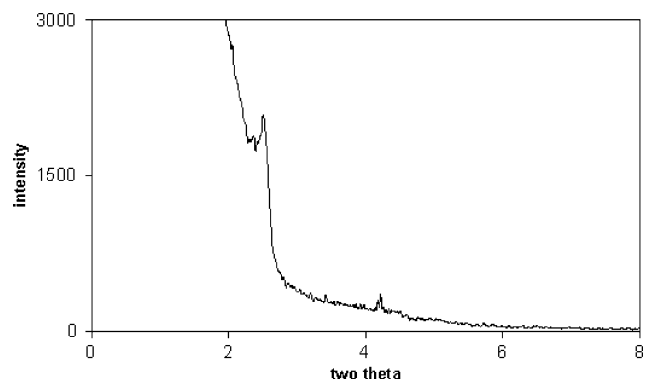


Fig. 2. XRD pattern of mesoporous Fe-AlPO calcined.

maximum intense peak, weakly resolved peaks corresponding to 1 1 0 and 2 0 0 reflections are also observed. These reflections are typical of a hexagonal lattice of MCM-41 type and characteristic of mesoporous materials. Fig. 3 represents

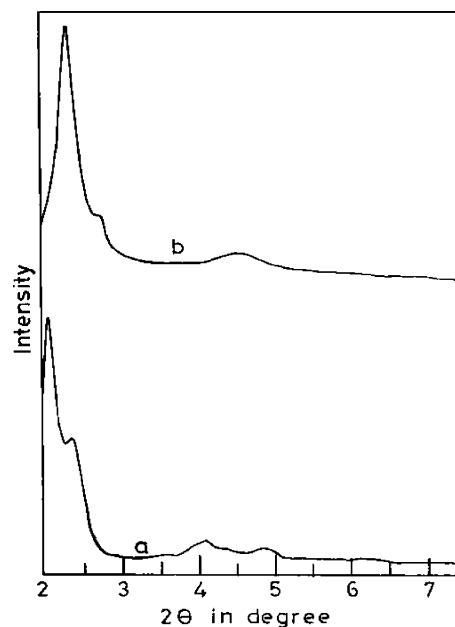


Fig. 3. XRD pattern of mesoporous Fe-MCM-48: (a) as-synthesized and (b) calcined.

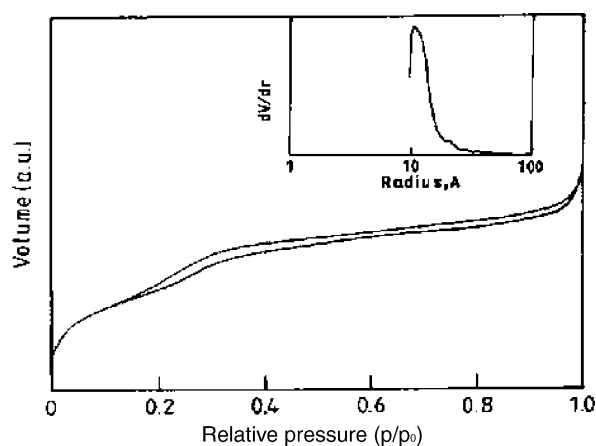


Fig. 4. N_2 adsorption isotherms of mesoporous Fe-AlPO.

the XRD pattern of mesoporous Fe-MCM-48, which shows clearly the formation of well-ordered cubic structure.

An organic base, TMAOH, is necessary to maintain the pH of the gel at 9.5, maintained at 9.5 as lower than pH 9.5 resulted in amorphous materials. It was observed that mild basic conditions are required to produce the hexagonal aluminophosphate [7,9]. To confirm this point, attempts were made to prepare the mesoporous aluminophosphates with other base sources like NaOH and NH_4OH . In both the cases, only amorphous materials resulted. Being stronger in nature, cations of these bases will have strong interaction with the inorganic assembly and thereby prevent the interaction of the later with the surfactant assembly. During the procedure employed, mesoporous AlPO resulted only at a pH > 9.0. Under the reaction conditions, more likely, a modified $S^+ - I^-$ ion-pair process is operative.

3.2. N_2 adsorption

Nitrogen adsorption–desorption data provide information regarding the porous nature and the surface area of the materials prepared. Fig. 4 represents the nitrogen adsorption–desorption isotherms of mesoporous Fe-AlPO recorded at liquid nitrogen temperature (77 K). Fe-AlPO has a BET surface area of $830 \text{ m}^2/\text{g}$ with an average pore size of $\sim 26 \text{ \AA}$. It was observed that Fe-AlPO exhibits type IV isotherm with a hysteresis loop in the region $p/p_0 = 0.2\text{--}0.4$ indicating mesoporous nature of the catalyst. This hysteresis loop is due to the capillary condensation, which is taking

place with in the mesopores. The values of BET surface area as well as average pore size distribution of both Fe-AlPO and Fe-MCM-48 are given in Table 1 together with other physico-chemical data.

3.3. Thermal analysis

Thermal analysis provides information regarding the removal of the surfactant and total weight loss after removal of the surfactant. Thermogram of mesoporous Fe-AlPO is given in Fig. 5, which shows three weight loss regions. The first one in the temperature <373 K is due to loss of physisorbed or weakly adsorbed water. The weight loss in the temperature range 373–623 K corresponds to the loss of surfactant. The final weight loss above 623 K is due to the loss of water due to condensation of the hydroxyl groups. In order to examine the thermal stability of mesoporous Fe-AlPO, calcination was performed at various temperatures and it was observed that mesoporous Fe-AlPO shows high thermal stability up to 973 K.

3.4. Optical spectral measurements

The location of the metal ions in different environments can be identified through UV–vis spectroscopy. UV–vis DRS spectra of as-synthesized and calcined mesoporous Fe-AlPO is given in Fig. 6. As-synthesized mesoporous Fe-AlPO shows only a band around 240 nm. Based on the earlier reports, this band was assigned to the ligand oxygen to metal iron charge transfer transition, indicating the presence of isolated FeO_4^- type species [11]. On calcination, the same band was retained indicating the presence of iron in the framework of mesoporous Fe-AlPO. On calcination bands corresponding to the extra framework iron oxide species were absent indicating the presence of the iron in the network of mesoporous Fe-AlPO.

3.5. ESR spectroscopy

ESR spectra of as-synthesized and calcined mesoporous Fe-AlPO are shown in Fig. 7. As-synthesized material at room temperature shows ESR spectrum with signals at $g = 4.3$ and 2.0. Based on the literature data, the first signal with $g = 4.3$ is assigned to Fe(III) in tetrahedral environment and the other signal at 2.0 is attributed to the presence of high spin Fe(III) in distorted tetrahedral/octahedral environments

Table 1
Physico-chemical data of Fe-substituted mesoporous materials

Catalyst	d [uncalc] (\AA)	d [calc.] (\AA)	a (\AA)	BET surface area (m^2/g)	Pore size (\AA)	Pore volume (cm^3/g)
AlPO	33.2	32.1	37.47 ^a	695	28	0.65
Fe-AlPO	35.8	34.74	40.56 ^a	820	28	0.61
MCM-48	33.7	32.9	80.50 ^b	1020	29	0.99
Fe-MCM-48	34.7	33.1	81.07 ^b	840	28	0.91

^a $a = 2d_{100}/3$.

^b $a = d_{211}\sqrt{(h^2 + k^2 + l^2)}$.

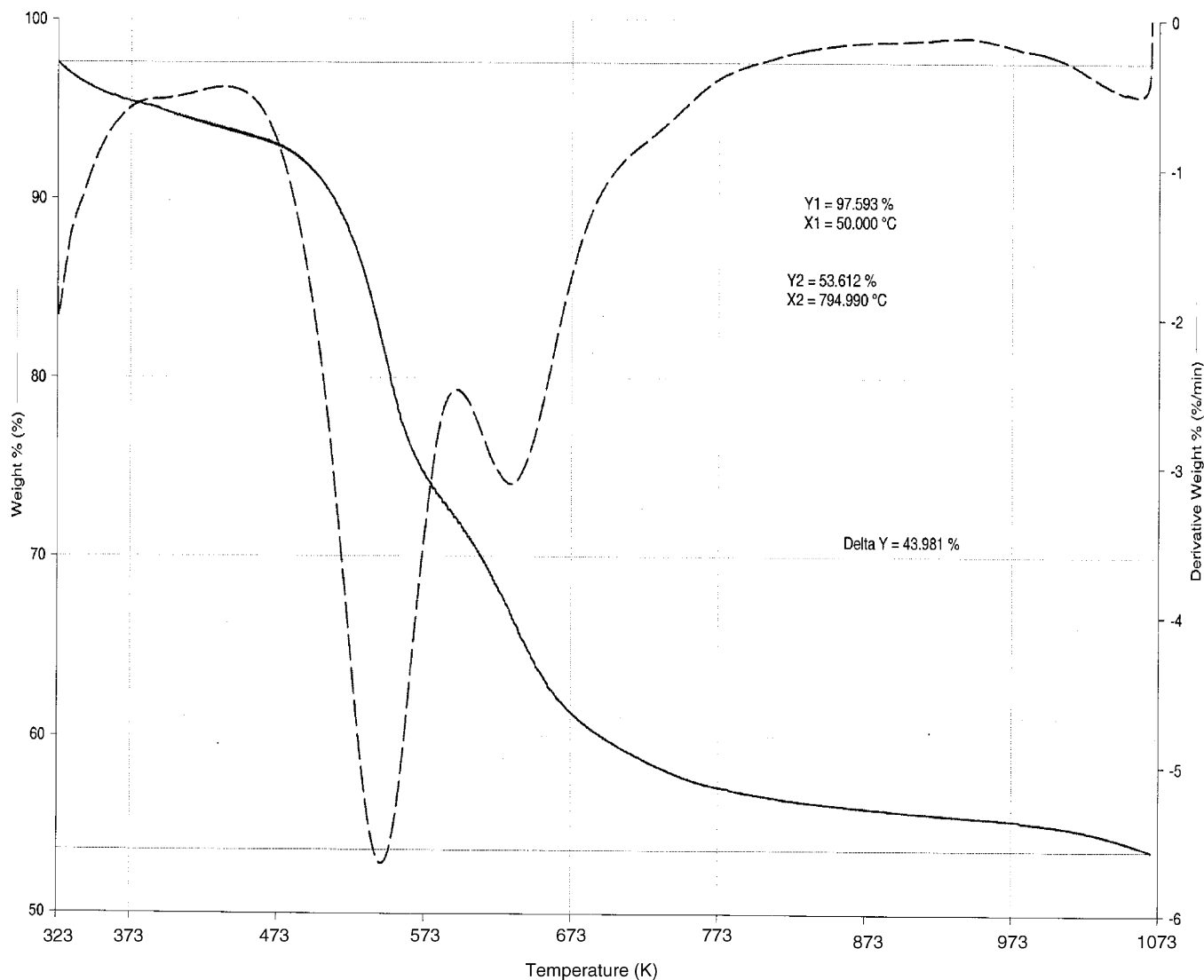


Fig. 5. TGA of mesoporous Fe-AIPO.

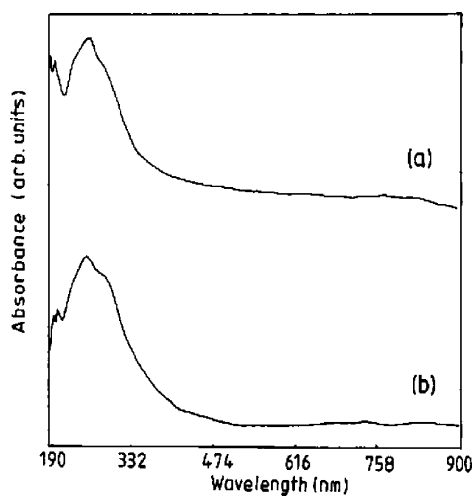


Fig. 6. UV-vis nujol spectra of mesoporous Fe-AIPO: (a) as-synthesized and (b) calcined.

[11]. The increase in intensity of $g = 4.3$ signal with decrease in temperature suggests that Fe(III) is in isolated tetrahedral location. Calcined Fe-AIPO also shows similar signals at $g = 4.3$ and 2.0. Interestingly, upon calcination, dislodging of

Table 2
Catalytic activity of mesoporous Fe-AIPO for oxidation of cyclohexane

Catalyst	Conversion (%)	Product selectivity (%)		
		Cyclohexanol	Cyclohexanone	Others ^a
Fe-AIPO	7.5	86.6	7.0	6.4
Fe-AIPO + 3 wt.% TBHP	14.2	92.0	3.7	4.3
Fe-AIPO + 3 wt.% HQ	1.4	68.0	29.6	–
Fe-MCM-48	1.3	> 99	–	–
Fe-AIPO ^b	7.7	87.2	6.1	6.7

Reaction conditions: pressure = 20 bar, $T = 403$ K, $t = 24$ h.

^a Unidentified products.

^b $P = 30$ bar.

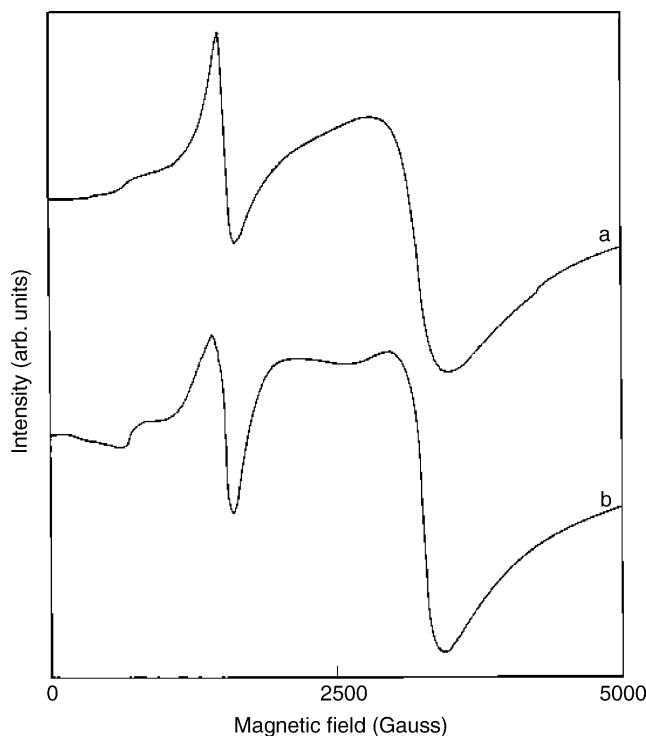


Fig. 7. ESR spectra of mesoporous Fe-AlPO: (a) as-synthesized and (b) calcined.

the iron from the framework was not observed indicating the absence of extra framework ferric oxide species after calcination. The assignment of the signals is also the same like uncalcined sample. In the case of calcined samples also, increase in intensity of the signals at 77 K was observed suggesting the presence of Fe(III) in isolated tetrahedral environment.

3.6. Oxidation of cyclohexane over mesoporous Fe-AlPO

Typical results on the aerial oxidation of cyclohexane over mesoporous Fe-AlPO and Fe-MCM-48 are given in Table 2. Liquid phase air oxidation of cyclohexane was carried out under high-pressure conditions (20, 30 bar) in a stainless steel autoclave at 403 K and the results indicate that Fe-AlPO is active for the cyclohexane oxidation and selective towards cyclohexanol. Under the reaction conditions employed mesoporous Fe-AlPO shows conversion of 7.5% with ~87% selec-

tivity towards cyclohexanol. In order to ensure the possibility of a reaction radical mechanism, a small amount (<3 wt.%) of radical initiator (70% TBHP) was added. Conversion of cyclohexane has increased to 14.2% retaining the selectivity to cyclohexanol. This increase in the conversion indicates that oxidation of cyclohexane is taking place through a radical mechanism. In order to confirm this further, the reaction was carried out with radical inhibitor hydroquinone. The decrease in the cyclohexane conversion to 1.3% further confirms the radical initiated mechanism.

4. Conclusions

Mesoporous Fe-AlPO analogous to uni-dimensional hexagonal MCM-41 was synthesized. Various physico-chemical techniques confirmed the formation of hexagonal mesoporous aluminophosphate and the presence of iron within the framework. Catalytic activity of synthesized mesoporous Fe-AlPO was tested for the aerial oxidation of cyclohexane under high-pressure conditions. The results indicated that the Fe-AlPO is an active catalyst for the oxidation of cyclohexane and the reaction is probably taking place through radical initiated mechanism.

References

- [1] S.T. Wilson, B.M. Lok, C.A. Messina, T.R. Cannan, E.M. Flanigen, *J. Am. Chem. Soc.* 104 (1982) 1176.
- [2] E.M. Flanigen, B.M. Lok, R.L. Patton, S.T. Wilson, *Proceedings of the 7th International Zeolite Conference*, Tokyo, Japan, 1986, p. 103.
- [3] J.M. Thomas, Robert Raja, *Chem. Commun.* (2001) 675.
- [4] T. Kresge, M.E. Leonowicz, W.J. Roth, J.C. Vartuli, J.S. Beck, *Nature* 359 (1992) 710.
- [5] B. Chakraborty, A.C. Pulikottil, S. Das, B. Viswanathan, *J. Chem. Soc., Chem. Commun.* (1997) 911.
- [6] M.P. Kapoor, Anuj Raj, *Appl. Catal. A* 203 (2000) 311.
- [7] D. Zhao, Z. Luan, L. Keven, *J. Chem. Soc., Chem. Commun.* (1997) 1009.
- [8] Ch. Subrahmanyam, B. Viswanathan, T.K. Varadarajan, *Eurasian ChemTech J.* 4 (2002) 169.
- [9] Ch. Subrahmanyam, B. Louis, F. Rainone, B. Viswanathan, A. Renken, T.K. Varadarajan, *Catal. Commun.* 3 (2002) 45.
- [10] Ch. Subrahmanyam, B. Louis, F. Rainone, B. Viswanathan, A. Renken, T.K. Varadarajan, *Appl. Catal. A: Gen.* 241 (2003) 205.
- [11] S.K. Mahapatra, B. Sahoo, W. Keune, P. Selvam, *Chem. Commun.* (2002) 1466.